Electronic Supplementary Information

Materials and methods

Unless otherwise stated, all materials were purchased from commercial sources and used as is.

Synthesis of 9-fluorenylpropanoic acid

9-fluorenylpropanoate methyl ester
A DMSO (20 ml) solution of fluorene (1.00 g, 6.0 mmol) was cooled to 0 ^{o}C in an ice bath, and stirred under nitrogen. To this was added 60% NaH dispersion in mineral oil (313 mg, 7.8 mmol), and the reaction mixture stirred for 40 minutes, before the subsequent addition of methyl 3-bromopropionate (985 µl, 9.0 mmol). After being allowed to warm to room temperature, the reaction mixture was stirred for a further hour, before being quenched by the slow addition of MeOH. The reaction mixture was then partitioned between DCM and 1 M HCl solution. The organic layer was isolated, dried over $MgSO_4$, and concentrated via rotary evaporation in order to afford the crude product. Purified by silica column chromatography, eluting with 2% MeOH/DCM in order to afford the title compound (297 mg, 19.6%).

9-fluorenylpropanoic acid
To a 1:1 THF/H_2O (10 ml) solution of 9-fluorenylpropanoate methyl ester (297 mg, 1.2 mmol) was added LiOH (125 mg, 3.0 mmol). The reaction mixture was stirred at room temperature for 2 hours. The reaction mixture was diluted with DCM, then washed with 1 M HCl (x2), water (x2), and brine. The organic layer was isolated and concentrated via rotary evaporation, in order to afford the title compound (260 mg, 92.7%).
^{1}H NMR ($CDCl_3$) δ 7.77 (d, 2H, ArH), 7.52 (d, 2H, ArH), 7.36 (m, 4H, ArH), 4.11 (t, 1H, ArCH), 2.46 (m, 2H, CH_2), 2.01 (m, 2H, CH_2)
^{13}C NMR ($CDCl_3$) δ 178.3 (COOH), 145.3 (ArH), 141.0 (ArH), 126.9 (ArH), 126.6 (ArH), 123.8 (ArH), 119.5 (ArH), 45.5 (ArCH), 28.5 (CH_2), 26.8 (CH_2)

Amide coupling example

9-Fluorenylmethyloxycarbonyl tyrosine leucine tert butyl ester
To a DCM (10 ml) solution of 9-Fluorenylmethyloxycarbonyl tyrosine (807 mg, 2.0 mmol) was added HCl.leucine tert butyl ester salt (671 mg, 3.0 mmol), DIPEA (1.43 ml, 8.3 mmol), and 50% T3P solution in EtOAc (1.85 ml, 3.0 mmol). The reaction mixture was stirred at room temperature for 1.5 hours. The reaction mixture was diluted with DCM, then washed with 1 M HCl (x2), water (x2), and brine. The organic layer was isolated and concentrated via rotary evaporation, in order to afford the crude product. Purified via silica column chromatography, eluting with a 0-2% MeOH/DCM gradient, in order to afford the title compound (796 mg, 70.1 %).

Tert butyl ester cleavage example

9-Fluorenylmethyloxycarbonyl tyrosine leucine
A 1:1 TFA/DCM (15 ml) solution of 9-Fluorenylmethyloxycarbonyl tyrosine leucine tert butyl ester (796 mg, 1.4 mmol) was stirred at room temperature for 3 hours. The reaction mixture was then concentrated via rotary evaporation. The residue was diluted with DCM, then washed with 1 M HCl (x2), water (x2), and brine. The organic layer was isolated, dried over $MgSO_4$, and concentrated via rotary evaporation, in order to afford the title compound (658 mg, 91.7%).
See characterisation below.

Final compound characterization summaries

9-fluorenylamide tyrosine leucine (1)
ESI MS $[M+Na]^+$ m/z 509.15, $[M-H]^-$ m/z 485.00
^{1}H NMR (CD_3OD) δ 7.78 (t, 2H, ArH), 7.47 (d, 1H, ArH), 7.39 (dt, 2H, ArH), 7.30 (t, 1H, ArH), 7.20 (t, 1H, ArH), 7.07 (d, 2H, ArH), 7.02 (d, 1H, ArH), 6.73 (d, 2H, ArH), 4.74 (m, 2H, ArCH/COCH), 4.48 (m, 1H, COCH), 3.16 (dd, 1H, $ArCH_2$), 2.86 (dd, 1H, $ArCH_2$), 1.66 (m, 3H, CH/CH_2), 0.94 (t, 6H, CH_3)

9-fluorenylacetamide tyrosine leucine (2)
ESI MS $[M+H]^+$ m/z 501.00, $[M+Na]^+$ m/z 523.16, $[M-H]^-$ m/z 499.14
^{1}H NMR (CD_3OD) δ 7.75 (dd, 2H, ArH), 7.35 (m, 3H, ArH), 7.24 (td, 1H, ArH), 7.20 (m, 2H, ArH), 7.14 (d, 2H, ArH), 6.73 (d, 2H, ArH), 4.83 (m, 1H, ArCH), 4.53 (m, 1H, CHCO), 4.31 (t, 1H, CHCO), 3.14 (dd, 1H, $ArCH_2$), 2.79 (dd, 1H, $ArCH_2$), 2.58 (qd, 2H, $ArCH_2$), 1.80 (m, 1H, CH), 1.70 (t, 2H, CH_2), 1.00 (dd, 6H, CH_3)

9-Fluorenylmethyloxycarbonyl tyrosine leucine (3)
ESI MS $[M+H]^+$ m/z 517.13, $[M+Na]^+$ m/z 539.20, $[M-H]^-$ m/z 514.87
^{1}H NMR (CD_3OD) δ 7.80 (d, 2H, ArH), 7.59 (d, 2H, ArH), 7.39 (t, 2H, ArH), 7.31 (q, 2H, ArH), 7.11 (d, 2H, ArH), 6.71 (d, 2H, ArH), 4.46 (t, 1H, ArCH), 4.39 (m, 1H, COCH), 4.32 (m, 1H, COCH), 4.18 (m, 2H, CH_2O), 3.08 (dd, 1H, CH_2Ar), 2.78 (dd, 1H, CH_2Ar), 1.67 (m, 3H, CH/CH_2), 0.94 (dd, 6H, CH_3)

9-fluorenylpropanamide tyrosine leucine (4)
ESI MS $[M+H]^+$ m/z 515.20, $[M+Na]^+$ m/z 537.27, $[M-H]^-$ m/z 513.20
^{1}H NMR (CD_3OD) δ 8.18 (1H, d, NH), 7.83 (1H, d, NH), 7.76 (d, 2H, ArH), 7.51 (dd, 2H, ArH), 7.32 (m, 4H, ArH), 7.01 (d, 2H, ArH), 6.65 (d, 2H, ArH), 4.54 (m, 1H, CHCO), 4.39 (m, 1H, CHCO), 3.94 (t, 1H, ArCH), 3.00 (dd, 1H, CH_2), 2.66 (dd, 1H, CH_2), 2.21 (m, 2H, CH_2), 1.87 (m, 2H, CH_2), 1.62 (m, 3H, CH/CH_2), 0.89 (dd, 6H, CH_3)

Formation of hydrogels

The peptide derivative was suspended in 1 ml of doubly distilled (ddH_2O), to give 20 mmol/L. For the physiological pH hydrogels; 93 mM of NaOH was added and the mixture sonicated to give a clear solution. 100 mM NaH_2PO_4 was added and the mixture vortexed briefly to give a 100 mM phosphate buffered hydrogel with a final pH of ~7.3. Throughout the NaOH/ NaH_2PO_4 addition, care was taken to ensure that the pH remained below 10.5 to prevent base catalysed loss of Fmoc functionality. The NaOH concentration can be decreased to achieve gelation for the lower pH systems, or alternatively the final pH can be adjusted by dropwise HCl addition. For FTIR samples, the above protocol was followed using deuterium oxide (D_2O) in place of water; though a negligible number of protons will be present from the non-deuterated NaOH, NaH_2PO_4, and the gelator compounds themselves.

HPLC

A Dionex P680 HPLC system equipped with a C18 column of 250 mm length, 4.6 mm internal diameter and 5mm particle size was also used to confirm >95% purity of final compounds. A gradient of 20% acetonitrile in water at 4 minutes to 80% acetonitrile at 31 minutes was used, with a flow rate of 1 ml/min and detection wavelength of 225 nm.

Rheology

To assess the mechanical properties of the hydrogels, dynamic frequency sweep experiments were carried out on a strain-controlled rheometer (Malvern Kinexus Pro) using a parallel-plate geometry (20 mm) with a 0.50 mm gap. To ensure the measurements were made in the linear viscoelastic regime, a strain sweep was performed. The dynamic modulus of the hydrogel was measured as a frequency function, where the frequency sweeps were carried out between 0.1 and 100 Hz. Note that at frequencies > 10 Hz, the extrusion of water and the consequently increased concentration of the samples, results in a sharp increase in the respective moduli values.

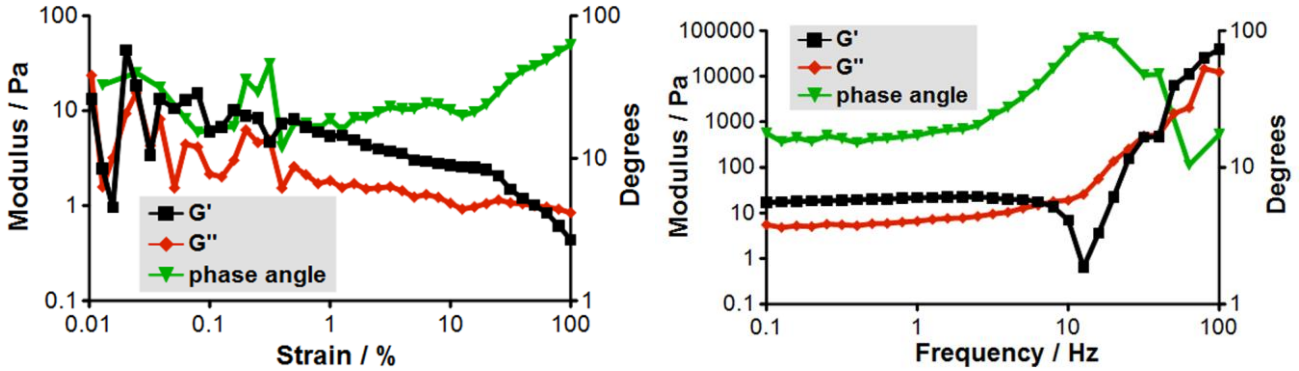

Figure S1. System **1** elastic (G') and viscous (G") moduli; [left] strain (@1 Hz) and [right] frequency (@1 %) sweeps

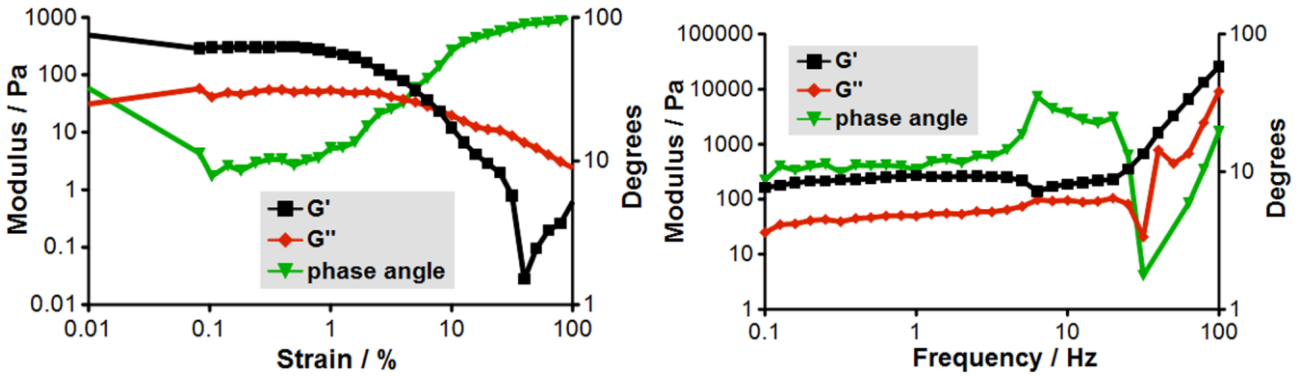

Figure S2. System **2** elastic (G') and viscous (G") moduli; [left] strain (@1 Hz) and [right] frequency (@0.2 %) sweeps

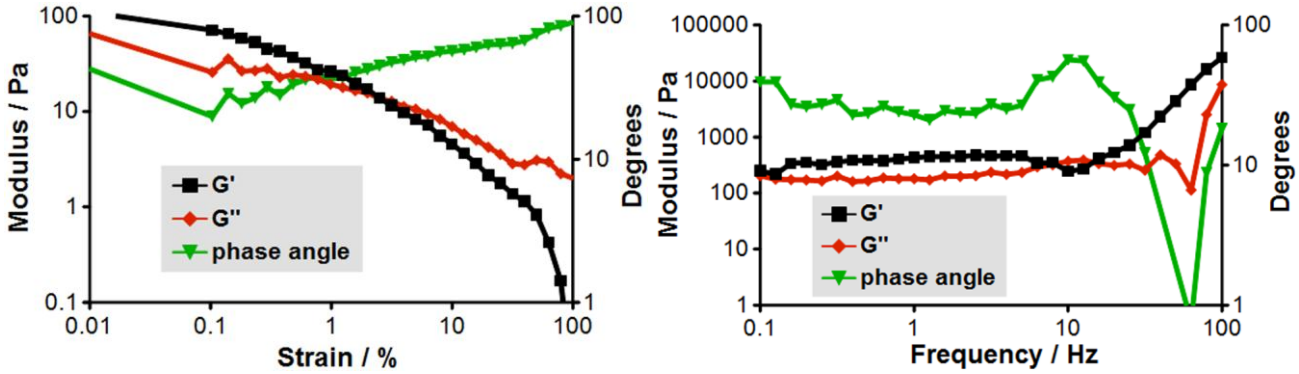

Figure S3. System **3** elastic (G') and viscous (G") moduli; [left] strain (@1 Hz) and [right] frequency (@0.2 %) sweeps

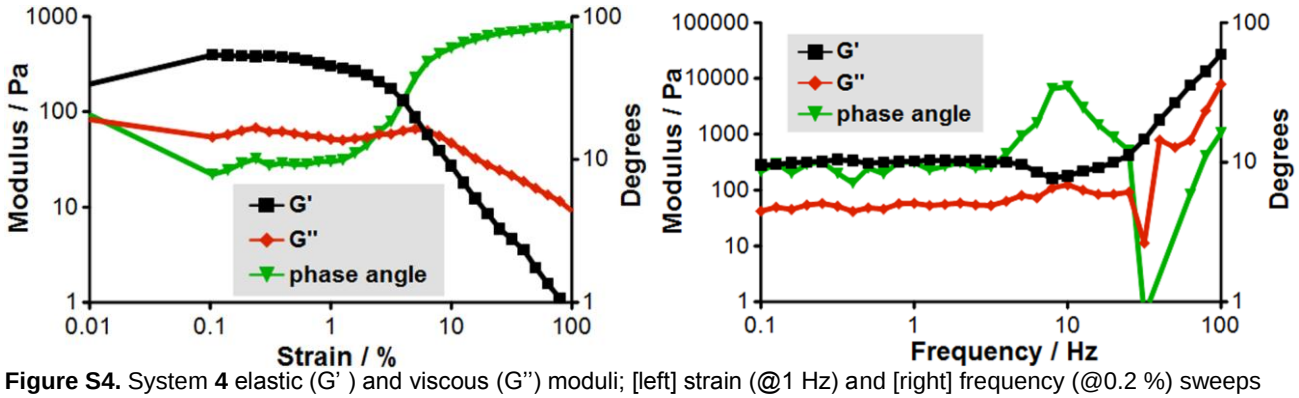

Figure S4. System **4** elastic (G') and viscous (G") moduli; [left] strain (@1 Hz) and [right] frequency (@0.2 %) sweeps

Fluorescence emission spectroscopy

Fluorescence emission spectra were measured on a Jasco FP-6500 spectrofluorometer, with emission measured perpendicular to the excitation light. 2 ml samples were transferred into cuvettes with a path length of 1 cm. An excitation wavelength of 295 nm was used, and the emission intensity recorded in the

range between 300 and 600 nm. An excitation and emission bandwidth of 3 nm was utilised, while the fluorometer sensitivity was altered to as to attain a well defined spectrum in each case.

Atomic force microscopy

20 µl of a 2 mM solution, was placed on a trimmed, freshly cleaved mica sheet attached to an AFM support stub, which was left to air-dry overnight in a dust-free environment, prior to imaging. The images were obtained by scanning the mica surface in air under ambient conditions using a Veeco MultiMode with NanoScope IIID Controller Scanning Probe Microscope (Digital Instruments, Santa Barbara, CA, USA; Veeco software Version 6.14r1) operated in tapping mode. The AFM measurements were obtained using a sharp silicon probe (TESP; nominal length (lnom) = 125 µm, width (wnom) = 40 µm, tip radius (Rnom) = 8 nm, resonant frequency (nom) = 320 kHz, spring constant (knom) = 42 N m-1; Veeco Instruments SAS, Dourdan, France), and AFM scans were taken at 512 x 512 pixels resolution. Typical scanning parameters were as follows: tapping frequency 308 kHz, integral and proportional gains 0.3 and 0.5, respectively, set point 0.5 – 0.8 V and scanning speed 1.0 Hz. The images were analysed using Veeco Image Analysis software Version 6.14r1.

Infrared absorption spectroscopy

Spectra were recorded on a Bruker Vertex 70 spectrometer, averaging 25 scans per sample at a resolution of 1 cm^{-1}. Samples were sandwiched between two 2 mm CaF_2 windows separated with a 25 µm PTFE spacer.

Circular dichroism

Samples were pipetted into a 0.2 mm cell. Spectra were measured between 200 and 400 nm on a Jasco J600 spectropolarimeter with 1 s integrations, a step size of 1 nm and a single acquisition with a slit width of 1 nm.

Other

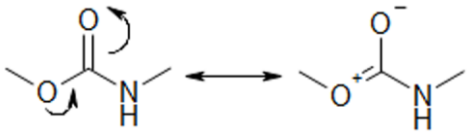

Figure S5. Resonance structure associated with the carbamate group

Linker flexibility computations

All calculations were performed at Density Functional Theory level in Gaussian09[1] employing the B3LYP functional and 6-31G(d,p) basis set. Structures **1-4** were geometry optimised and frequency calculations were performed to extract molecular entropy. Subsequently, the relevant dihedral angles were changed in 20° steps and single point energy calculations (no re-optimisation) were performed to obtain a frozen potential energy curve. Note that no significant additional interactions were present between fluorene ring atoms and the rest of the molecule when the dihedral was changed.

Table S1. DFT calculated vibrational, translational and rotational contributions to total entropy for entries **1-4**. All values are in cal mol^{-1} K^{-1}.

	S_{total}	S_{vib}	S_{trans}	S_{rot}
1	171.6	92.1	43.5	36.1
2	178.0	98.0	43.6	36.4
3	184.6	104.1	43.7	36.8
4	186.0	105.4	43.7	37.0

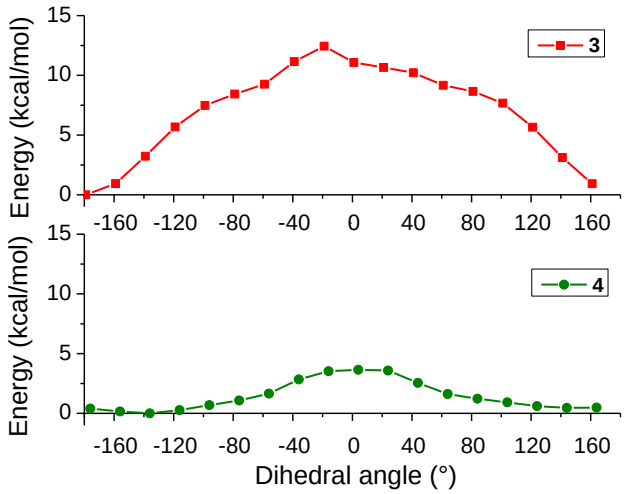

Figure S6. Calculated potential energy as a function of the *φ* dihedral angle (see main text Fig. 1) of **3** (measured N-C-O-C) and **4** (measured N-C-C-C). The lowest energy is set as 0.

ESI reference

1. Gaussian 09, Revision A.02, Frisch, M. J.; Trucks, G. W.; Schlegel, H. B.; Scuseria, G. E.; Robb, M. A.; Cheeseman, J. R.; Scalmani, G.; Barone, V.; Mennucci, B.; Petersson, G. A.; Nakatsuji, H.; Caricato, M.; Li, X.; Hratchian, H. P.; Izmaylov, A. F.; Bloino, J.; Zheng, G.; Sonnenberg, J. L.; Hada, M.; Ehara, M.; Toyota, K.; Fukuda, R.; Hasegawa, J.; Ishida, M.; Nakajima, T.; Honda, Y.; Kitao, O.; Nakai, H.; Vreven, T.; Montgomery, Jr., J. A.; Peralta, J. E.; Ogliaro, F.; Bearpark, M.; Heyd, J. J.; Brothers, E.; Kudin, K. N.; Staroverov, V. N.; Kobayashi, R.; Normand, J.; Raghavachari, K.; Rendell, A.; Burant, J. C.; Iyengar, S. S.; Tomasi, J.; Cossi, M.; Rega, N.; Millam, J. M.; Klene, M.; Knox, J. E.; Cross, J. B.; Bakken, V.; Adamo, C.; Jaramillo, J.; Gomperts, R.; Stratmann, R. E.; Yazyev, O.; Austin, A. J.; Cammi, R.; Pomelli, C.; Ochterski, J. W.; Martin, R. L.; Morokuma, K.; Zakrzewski, V. G.; Voth, G. A.; Salvador, P.; Dannenberg, J. J.; Dapprich, S.; Daniels, A. D.; Farkas, Ö.; Foresman, J. B.; Ortiz, J. V.; Cioslowski, J.; Fox, D. J. Gaussian, Inc., Wallingford CT, 2009.